# CHARACTERISATION OF $Al_2O_3$ AND SrO MODIFIED $LaMnO_3$ FOR SOFC CATHODE MATERIAL

Danjela Kuščer, Janez Holc, Marko Hrovat, Slavko Bernik, Drago Kolar
Jožef Stefan Institute, Ljubljana, Slovenia

**Keywords**: SOFC, Solid Oxide Fuel Cells, high temperature SOFC, high temperature fuel cells with solid oxide electrolyte, lanthanum manganites, doping, microstructures, electrical resistivity, cathode materials, anode materials, solid electrolytes, YSZ, Yttrium Stabilized cubic Zirconium, environmental friendly, power generation, semiconducting perovskites, TEC, Thermal Expansion Coefficients, XRD analysis, X-Ray Diffraction analysis, EDS microanalysis, Energy Disperse x-ray System microanalysis

**Abstract:** The perovskites with nominal compositions $La(Mn_{1-x}Al_x)O_3$, strontium doped $(La_{0.8}Sr_{0.2})(Mn_{1-x}Al_x)O_3$ (for x between 0 and 0.94), and substoichiometric $(La_{0.8}Sr_{0.2})_{0.95}(Mn_{0.7}Al_{0.3})O_3$ were evaluated as possible solid oxide fuel cell (SOFC) cathodes. Cell parameters of solid solutions were calculated. The electrical and microstructural characteristics and high temperature interactions with yttria stabilised zirconia (YSZ) were studied. As compared with "pure" perovskites, doping with strontium and aluminum decreases and increases their specific resistivity, respectively. The incorporation of alumina substantially reduces the sinterability resulting in a rather porous, fine grained microstructure. The partial exchange of lanthanum with strontium and manganese with aluminum oxide significantly depress the reaction rate between perovskites and YSZ.

# Karakterizacija $LaMnO_3$, modificiranega z $Al_2O_3$ in SrO, za katodni material za SOFC

**Ključne besede:** SOFC celice gorivne z elektroliti oksidnimi trdnimi, SOFC celice gorivne z elektroliti oksidnimi trdnimi visootemperaturne, manganiti lantanovi, dopiranje, mikrostrukture, upornost električna, materiali katodni, materiali anodni, elektroliti trdni, YSZ cirkonij kubični stabiliziran z itrijem, okolno prijazno, proizvodnja energije, perovskiti polprevodni, TEC koeficienti razteznosti termičnih, XRD analiza z uklonom Rentgen žarkov, EDS mikroanaliza z energijsko razpršenimi Rentgen žarki

**Povzetek:** Kot možne materiale za visokotemperaturne gorivne celice s trdnim elektrolitom (SOFC) smo sintetizirali in karakterizirali perovskite z nominalnimi sestavami $La(Mn_{1-x}Al_x)O_3$, s stroncijem dopirane $(La_{0.8}Sr_{0.2})(Mn_{1-x}Al_x)O_3$ (x med 0 in 0.94), in podstehiometričnega $(La_{0.8}Sr_{0.2})_{0.95}(Mn_{0.7}Al_{0.3})O_3$. Izračunali smo dimenzije osnovnih celic trdnih raztopin. Študirali smo električne in mikrostrukturne karakteristike ter visokotemperaturne interakcije s trdnim elektrolitom. Zamenjava dela mangana z aluminijem poveča specifične upornosti, medtem ko zamenjava dela lantana s stroncijem upornosti zmanjša. Obe vrsti dopiranja zelo zmanjšata reaktivnost med testiranimi perovskiti in trdnim elektrolitom.

## INTRODUCTION

A fuel cell is a device for direct conversion of chemical energy into electrical energy. Basicaly it consists of cathode, anode and electrolyte. Oxidant is fed to the cathode and reducent (fuel) to the anode. The electrolyte, through which the ion current flows, prevents the mixing of oxidant and fuel. The concept is nearly 160 years old. The principle of fuel cell operation was reported in 1839 by Sir William Grove /1/. His fuel cell used dilute acid as an electrolyte and oxygen and hydrogen as oxidant and reducent, respectively.

High temperature fuel cells with a solid oxide electrolyte (SOFC) work at temperatures around 1000°C. Due to the high operating temperatures the choice of materials is limited mainly to ceramics. The solid electrolyte in SOFC cells is usually yttria stabilised cubic zirconia (YSZ). Cathodes are semiconducting perovskites and anodes are based on the mixture of metallic Ni and YSZ. An extensive and comprehensive review of materials for SOFC is presented in references /2,3/.

The oxygen accepts electrons at the cathode and moves as an ion through the dense $ZrO_2$ ceramic. At the anode ions combine with fuel and release electrons. The "force" driving oxygen ions through the electrolyte is the concentration gradient of oxygen between the cathode and the anode side. The fuel is hydrogen, a $H_2$/CO mixture, or hydrocarbons because the high operating temperature enables the internal (in situ) reforming of hydrocarbons with water vapour /4-6/. For the typical "working" conditions of an SOFC the open circuit voltage is around 1 V.

The advantage of high temperature solid oxide fuel cells for production of electrical energy is their high efficiency of 50-60%, while some estimates are even up to a yield of 70-80%. Also, nitrous oxides are not produced and the amount of $CO_2$ released per kWh, due to the high efficiency, is around 50 percent less than for power sources based on combustion, making SOFC "environmental friendly" power generation /7-11/.

The schematic diagram of the solid oxide fuel cell is shown in Fig. 1. Oxidant (air) is fed to the cathode and reductant (fuel) to the anode. The electrode reactions (for hydrogen as fuel) are:

Cathode: $1/2\ O_2 + 2\ e^- \longrightarrow O^{2-}$

Anode: $H_2 + O^{2-} \longrightarrow H_2O + 2\ e^-$

The crossections of two basic constructions of SOFC, tubular and planar, are shown schematically in Figs. 2 and 3, respectively. Fuel cell elements - anode/solid

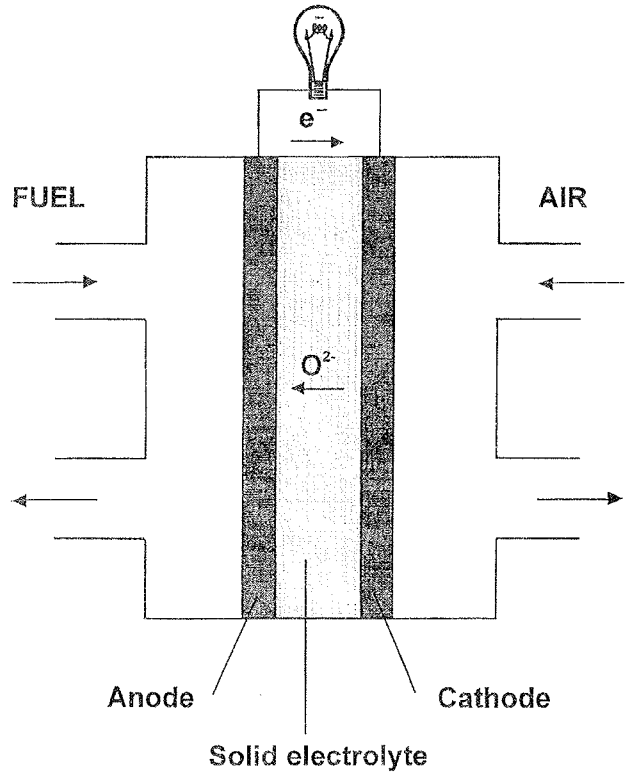


*Fig. 1. Schematic diagram of the solid oxide fuel cell (SOFC). Air is fed to the cathode and fuel to the anode. The electrolyte, through which the ion current is flowing, also prevents the mixing of oxidant and fuel.*

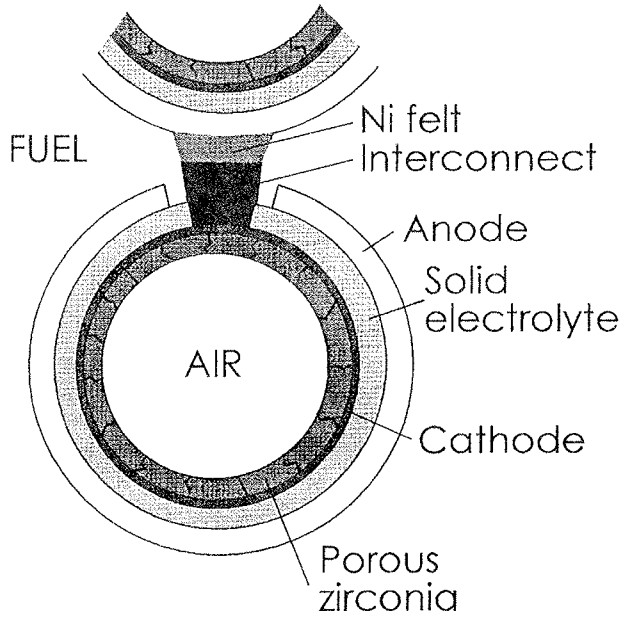


*Fig. 2: Crossection of the tubular design of a SOFC (schematically). The porous cathode and its coating of dense solid electrolyte are deposited on the porous $ZrO_2$ based carrier tube. Electrical contact with the anode of the next cell is obtained with nickel felt. Air flows through carrier tube and the fuel flows between the tubes.*

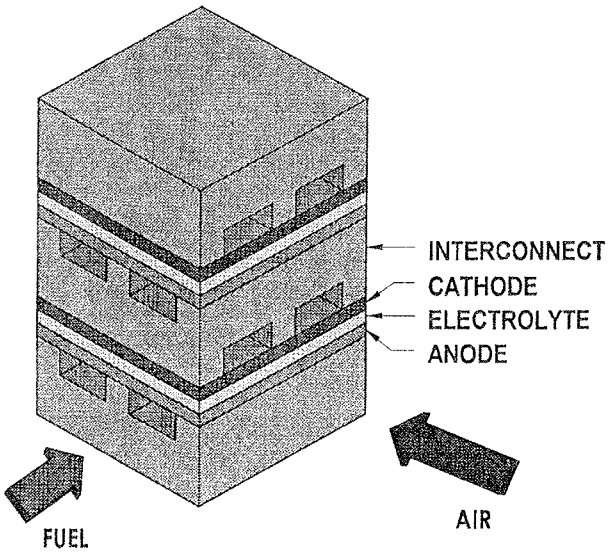


*Fig. 3: Crossection of the planar design of a SOFC (schematically). The air and the fuel flow through channels in the interconnect.*

electrolyte/cathode "sandwiches" are serially connected with an interconnect. Electrical charge flows as electrons through the interconnect and as oxygen ions through the solid electrolyte. In the case of tubular design air flows inside tubes over the cathode and fuel on the outside over anode while in the case of planar design air and fuel are flowing through the channels in the interconnect.

Cathode (air electrode) materials, which must withstand high operating temperatures and an oxidizing atmosphere, are at present based mostly on $LaMnO_3$ perovskites, doped with alkaline earth oxides, mainly SrO, to decrease specific resistivity. The thermal expansion coefficients (TEC) of $LaMnO_3$ is close enough to that of YSZ ($11.2 \times 10^{-6}$/K and $10.5 \times 10^{-6}$/K, respectively), to prevent cracking or delamination of SOFC components either during high temperature operation or heating / cooling cycles /2,12,13/. Also, SOFC cathode materials must be porous to allow the diffusion of oxygen from the air to the solid electrolyte.

It is known that lanthanum perovskites, with the possible exception of $LaCrO_3$ /14/, react during high temperature ageing with zirconia from YSZ solid electrolyte, forming $La_2Zr_2O_7$ pyrochlore /15-19/. The specific electrical resistivity of $La_2Zr_2O_7$ is three to four orders of magnitude higher than that of $LaMnO_3$ (reported to be $1.5 \times 10^3$ ohm.cm /17/, or even $25 \times 10^3$ ohm.cm /20/ at 1000°C), which increases the cell losses and therefore decrease its yield due to increased internal resistivity.

In this paper an evaluation of the electrical and microstructural characteristics of $La(Mn_{1-x}Al_x)O_3$ and strontium doped $(La_{0.8}Sr_{0.2})(Mn_{1-x}Al_x)O_3$ (for x between 0 and 0.94) based materials as possible SOFC cathode materials is described. A range of solid solutions exists between $LaMnO_3$ and $LaAlO_3$ which enables some "tailoring" of material characteristics /21/. Although the

alumina-rich perovskites, i.e. x=0.94, are not interesting for SOFC cathodes due to their high specific resistivities, they are included to cover the entire $Al_2O_3$ concentration range. The literature data show that substoichiometry on "A" sites suppresses the reactivity with YSZ (see, for example, /18/) therefore some results on substoichiometric $(La_{0.8}Sr_{0.2})_{0.95}(Mn_{0.7}Al_{0.3})O_3$ will be also presented.

## EXPERIMENTAL

For experimental work, $La(OH)_3$ (Ventron, 99.9%), $SrCO_3$ (Ventron, 99.9%), $MnO_2$ (Ventron, 99.9%), and $Al_2O_3$ (Alcoa, A-16, +99%) were used. The compositions of the samples were $La(Mn_{1-x}Al_x)O_3$ and $(La_{0.8}Sr_{0.2})_{0.95}(Mn_{1-x}Al_x)O_3$ (for "x" between 0 and 0.94) and $(La_{0.8}Sr_{0.2})_{0.95}(Mn_{0.7}Al_{0.3})O_3$. The samples were mixed in isopropyl alcohol, pressed into pellets, calcined at 1000°C and fired for 50 hours with intermediate grinding at 1200°C for $La(Mn_{1-x}Al_x)O_3$ and at 1300°C for strontium doped perovskites. During firing pellets were placed on platinum foils. To study the possible interactions at elevated temperatures, perovskites and YSZ powders were mixed in 1:1 molar ratio, pressed into pellets and fired at 1400°C for 300 hours. Samples were placed on platinum foils in alumina crucibles. The results were evaluated by XRD (X-ray powder diffraction analysis), SEM (scanning electron microscopy) and EDS (Energy Dispersive X-ray Microanalysis).

A JEOL JXA-840 scanning electron microscope equipped with a Tracor-Northern energy dispersive system (EDS) was used for overall microstructural and compositional analysis. Samples prepared for SEM were mounted in epoxy in cross-sectional orientation and then polished using standard metallographic techniques. Prior to analysis in the SEM, the samples were coated with carbon to provide electrical conductivity and avoid charging effects. In the case of standardless analysis the Tracor SQ standardless quantitative analysis program using multiple least-squares analysis and ZAF matrix correction procedure was used. Samples were analyzed under the following conditions: acceleration voltage 25 kV; probe current 250 pA; spectra acquisition time 100 s.

The phases in the sintered samples were determined using a Philips X-ray powder diffractometer using $CuK_\alpha$ radiation at a step size of 0.02° in the range $2\theta = 20°$ to 70°.

Electrical d.c. resistance was measured with four point method on sintered pellets with diameter of 6 mm and thickness of 2 mm with a Keithley 196 multimeter and a Keithley 580 Micro-ohmmeter instrument in the temperature range 20 - 925°C in air. Unfritted Pt electrodes were deposited as contacts on both sides of the samples and fired for 30 minutes at 1100 °C.

## RESULTS AND DISCUSSION

The microstructures of $La(Mn_{1-x}Al_x)O_3$, $(La_{0.8}Sr_{0.2})(Mn_{1-x}Al_x)O_3$, and $(La_{0.8}Sr_{0.2})_{0.95}(Mn_{0.7}Al_{0.3})O_3$ are in Figs. 4, 5, and 6, respectively. The microstructures are porous and average grain diameters decrease with increasing $Al_2O_3$ content.

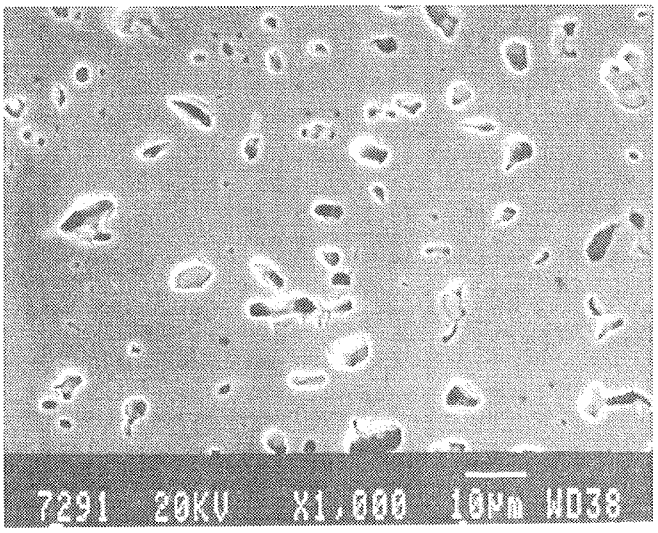


*Fig. 4.a: The microstructure of $LaMnO_3$*

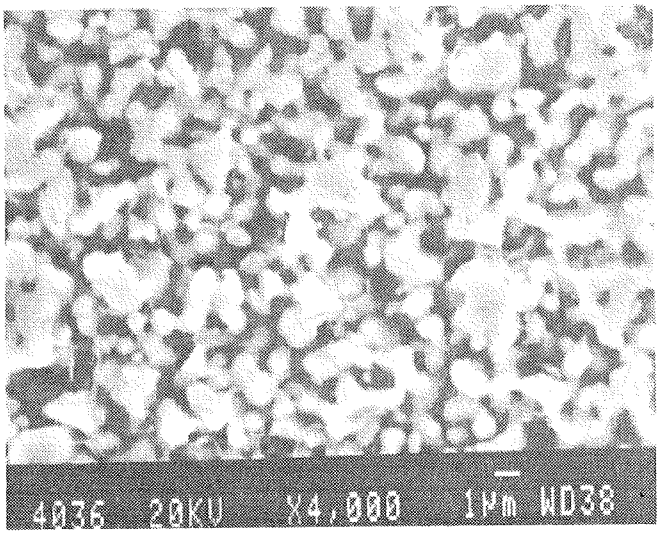


*Fig. 4.b: The microstructure of $La(Mn_{0.8}Al_{0.2})O_3$*

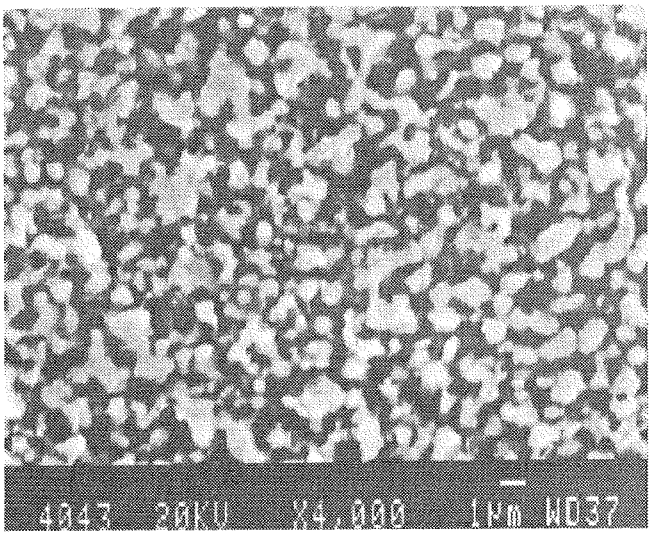


*Fig. 4.c: The microstructure of $La(Mn_{0.5}Al_{0.5})O_3$*

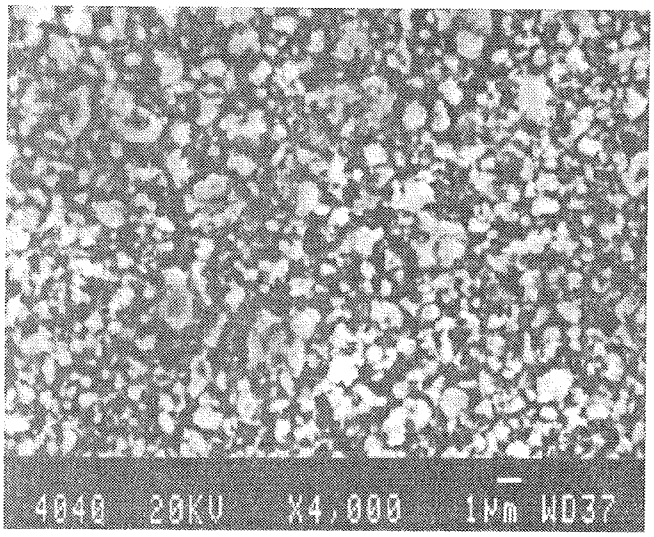


*Fig. 4.d: The microstructure of $La(Mn_{0.06}Al_{0.94})O_3$*

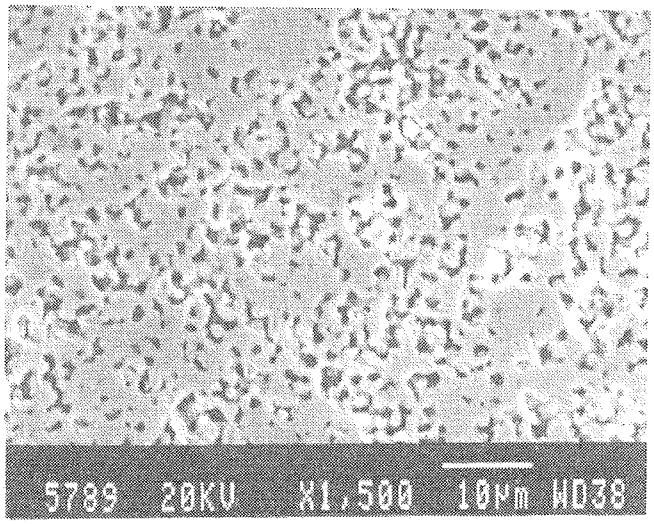


*Fig. 5.b: The microstructure of $(La_{0.8}Sr_{0.2})(Mn_{0.7}Al_{0.3})O_3$*

The microstructure of $La_{0.8}Sr_{0.2}MnO_3$ is well sintered (Fig. 5.a), but more porous than that of $LaMnO_3$ (Fig. 4.a). Data in the literature indicate that the partial replacement of the lanthanum with the strontium increased the density of sintered materials up to 10% substitution. For higher concentrations the densities of sintered samples decrease /22/. Substoichiometry on "A" sites increases the sintered density (Fig. 5.b - stoichiometric $(La_{0.8}Sr_{0.2})(Mn_{0.7}Al_{0.3})O_3$. and Fig. 6 - substoichiometric $(La_{0.8}Sr_{0.2})_{0.95}(Mn_{0.7}Al_{0.3})O_3$. Dark gray inclusions in Fig. 5.d (alumina rich $(La_{0.8}Sr_{0.2})(Mn_{0.06}Al_{0.94})O_3$ composition) are, according to the results of X-ray analysis and EDS microanalysis, $LaSrAlO_4$ compound.

In Table I and Table II the calculated cell parameters of $La(Mn_{1-x}Al_x)O_3$ and $(La_{0.8}Sr_{0.2})(Mn_{1-x}Al_x)O_3$ solid solutions, respectively, are given. Cell parameters were calculated from uncalibrated X-ray powder diffractometer data using the PARAM program. $LaMnO_3$, $LaAlO_3$ and solid solutions are indexed by a hexagonal cell, only $La_{0.8}Sr_{0.2}MnO_3$ is indexed by monoclinic cell. The

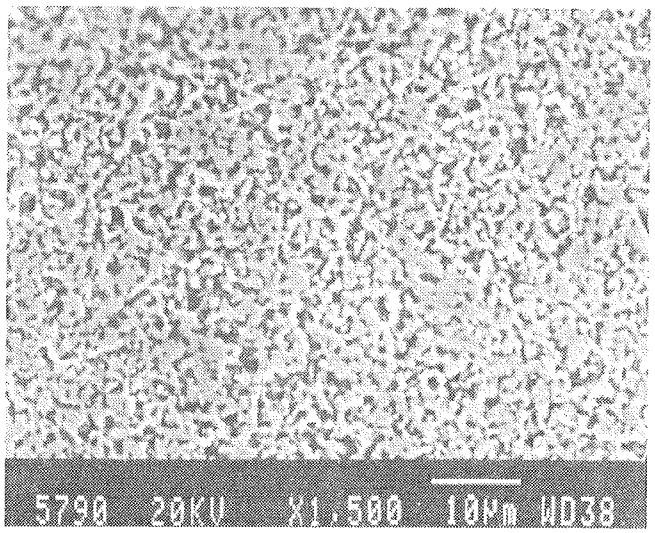


*Fig. 5.c: The microstructure of $(La_{0.8}Sr_{0.2})(Mn_{0.5}Al_{0.5})O_3$*

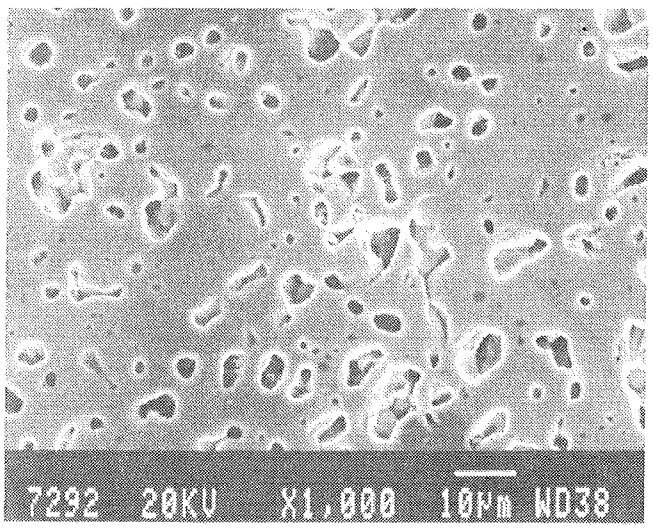


*Fig. 5.a: The microstructure of $(La_{0.8}Sr_{0.2})MnO_3$*

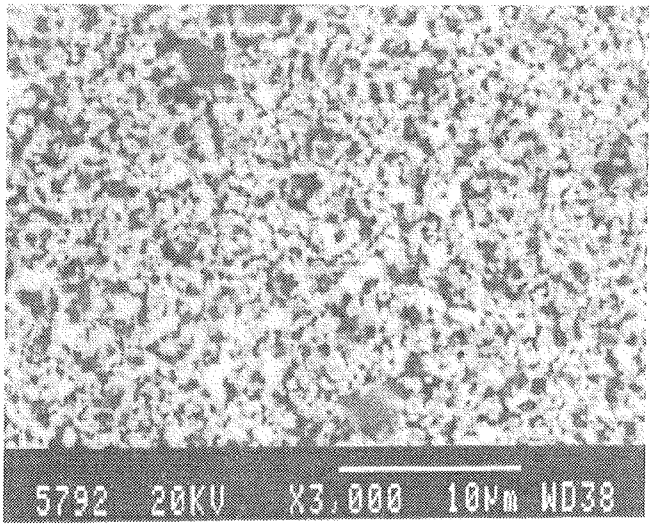


*Fig. 5.d: The microstructure of $(La_{0.8}Sr_{0.2})(Mn_{0.06}Al_{0.94})O_3$*

number in the bracket indicates the accuracy of the last significant digit. Subunit cell volumes are also shown in Fig. 7. Vertical bars indicate the accuracy of the calculated volume of perovskite subunit cells (the volume of unit cells in Table I and in Table II, divided by the number of subunit cells or pseudo-cells in the unit cell, i.e. 4 in the case of a monoclinic cell and 6 in the case of a hexagonal cell).

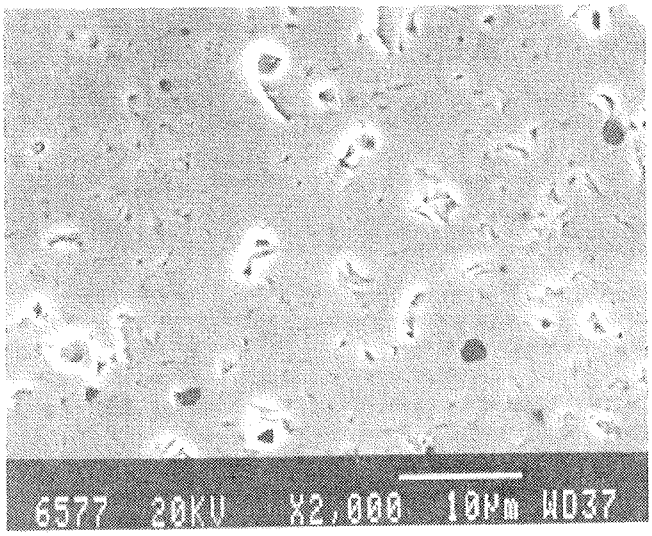


*Fig. 6: The microstructure of substoichiometric $(La_{0.8}Sr_{0.2})_{0.95}(Mn_{0.7}Al_{0.3})O_3$*

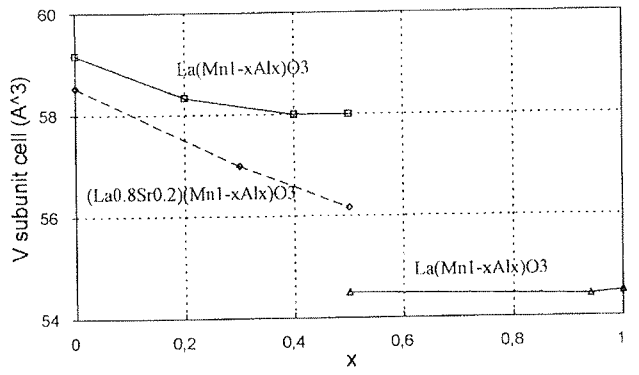


*Fig. 7: Volume of perovskite subunit (or pseudo-) cells vs. composition for $La(Mn_{1-x}Al_x)O_3$ and strontium substituted $(La_{0.8}Sr_{0.2})(Mn_{1-x}Al_x)O_3$.*

The values obtained for $LaMnO_3$, $LaAlO_3$, and $La_{0.8}Sr_{0.2}MnO_3$ are in fair agreement with data in JCPDS-ICDD 32-484, JCPDS-ICDD 31-22, and JCPDS-ICDD 40-1100 cards, respectively. The cell volume of $La(Mn_{1-x}Al_x)O_3$ linearly decreases with increasing alumina content from x=0 to x=0.4 which is the limit of solid solubility of $LaAlO_3$ in $LaMnO_3$ at 1200°C. It is due to the smaller ionic radius of $Al^{3+}$ ($Al^{3+}$ 0.535 Å and $Mn^{3+}$ 0.645 Å). Strontium substituted perovskites $(La_{0.8}Sr_{0.2})(Mn_{1-x}Al_x)O_3$ have smaller cell volumes as their counterparts with the same aluminum / manganese ratio. The ionic radius of $Sr^{2+}$ and $La^{3+}$ are similar ($La^{3+}$ 1.36 Å and $Sr^{2+}$ 1.44 Å), therefore the contraction of volume occurs either due to formation of oxygen vacancies or smaller $Mn^{4+}$ ions ($Mn^{4+}$=0.53 Å). Oxygen vacancies and/or $Mn^{4+}$ ions are needed for charge compensation when the $La^{3+}$ ion on "A" site is exchanged by the lower valence $Sr^{2+}$ ion.

*Table 1: Calculated cell parameters for materials with nominal compositions $La(Mn_{1-x}Al_x)O_3$*

| Nominal composition | a(Å) | c(Å) | V(Å$^3$) |
|---|---|---|---|
| $LaMnO_3$ | 5.531(5) | 13.38(2) | 355(1) |
| $La(Mn_{0.8}Al_{0.2})O_3$ | 5.512(4) | 13.29(2) | 350(1) |
| $La(Mn_{0.6}Al_{0.2})O_3$ | 5.502(5) | 13.27(2) | 348(1) |
| $La(Mn_{0.5}Al_{0.5})O_3$ * | 5.497(7) | 13.29(3) | 348(2) |
| $La(Mn_{0.5}Al_{0.5})O_3$** | 5.368(2) | 13.12(3) | 327(1) |
| $La(Mn_{0.06}Al_{0.94})O_3$ | 5.3630(9) | 13.11(1) | 326.6(4) |
| $LaAlO_3$ | 5.363(1) | 13.5(2) | 327(7) |

* solid solution of $Al_2O_3$ in $LaMnO_3$

** solid solutions of $Mn_2O_3$ in $LaAlO_3$

Specific electrical resistivities are given for "as fired" samples and are not corrected for porosity of materials. The logarithm of resistivities of $La(Mn_{1-x}Al_x)O_3$ vs. reciprocal temperature is shown in Fig. 8. The logarithm of resistivities of $La(Mn_{1-x}Al_x)O_3$ vs. "x", i.e., alumina content is shown in Fig. 9 for 700°C and 900°C. Specific resistivities increase with increasing concentration of

*Table 2: Calculated cell parameters for materials with nominal compositions $(La_{0.8}Sr_{0.2})(Mn_{1-x}Al_x)O_3$*

| nominal composition | a(Å) | b(Å) | c(Å) | β(°) | V(Å$^3$) |
|---|---|---|---|---|---|
| $La_{0.8}Sr_{0.2}MnO_3$ | 5.479(3) | 5.523(3) | 7.74(2) | 90.5(1) | 234.1(9) |
| $La_{0.8}Sr_{0.2}Mn_{0.7}Al_{0.3}O_3$ * | 5.457(4) | | 13.25(2) | | 342(1) |
| $La_{0.8}Sr_{0.2}Mn_{0.5}Al_{0.5}O_3$ | 5.413(3) | | 13.27(3) | | 337(1) |
| $La_{0.8}Sr_{0.2}Mn_{0.06}Al_{0.94}O_3$ | 5.28(4) | | 13.2(2) | | 319(9) |

* monoclinic cell

$Al_2O_3$. The change of slope in the resistivity vs. alumina content curves (Fig. 9) at x=0.4 is presumably due to the limit of solid solution in the $LaMnO_3$ rich region /21/.

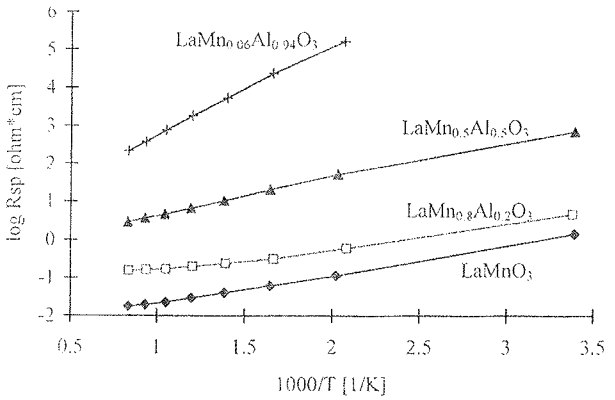


*Fig. 8: The logarithm of resistivities of $La(Mn_{1-x}Al_x)O_3$ vs. reciprocal temperature*

The logarithm of resistivities of $(La_{0.8}Sr_{0.2})(Mn_{1-x}Al_x)O_3$ vs. reciprocal temperature is shown in Fig. 10. The resistivity of $LaMnO_3$ is presented for comparison. The resistivities of $LaMnO_3$ and $(La_{0.8}Sr_{0.2})(Mn_{1-x}Al_x)O_3$ for x=0 and 0.3 are nearly the same for the whole temperature range at temperatures over 200°C, whereas for x=0.5 the resistivity is higher by an order of magnitude. The specific resistivities of $(La_{0.8}Sr_{0.2})(Mn_{0.7}Al_{0.3})O_3$ are comparable or even slightly lower than the resistivities of $(La_{0.8}Sr_{0.2})MnO_3$ (without alumina).

For comparison, the resistivities of undoped $La(Mn_{1-x}Al_x)O_3$ samples and SrO doped $(La_{0.8}Sr_{0.2})(Mn_{1-x}Al_x)O_3$ samples are plotted together in Fig. 11. The resistivities of strontium doped samples are about one order of magnitude lower than those of undoped samples. While the resistivity of undoped $La(Mn_{0.7}Al_{0.3})O_3$ is an order of magnitude higher than the resistivity of $LaMnO_3$, for SrO doped samples the resistivities of similar compositions, i.e., $(La_{0.8}Sr_{0.2})MnO_3$ and $(La_{0.8}Sr_{0.2})(Mn_{0.7}Al_{0.3})O_3$ are nearly the same.

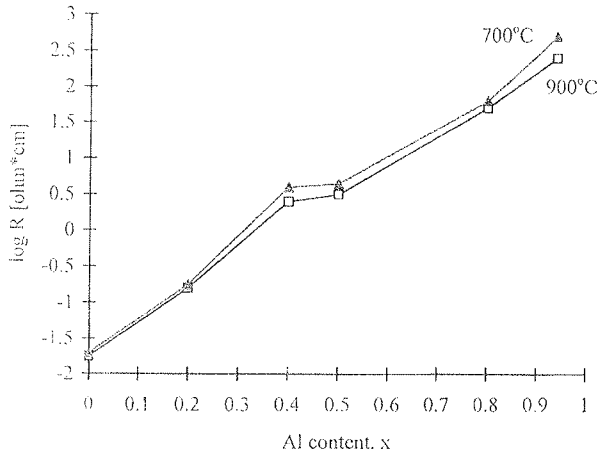


*Fig. 9: Logarithm of specific resistivities of $La(Mn_{1-x}Al_x)O_3$ at 700°C and 900°C as a function of $Al_2O_3$ content.*

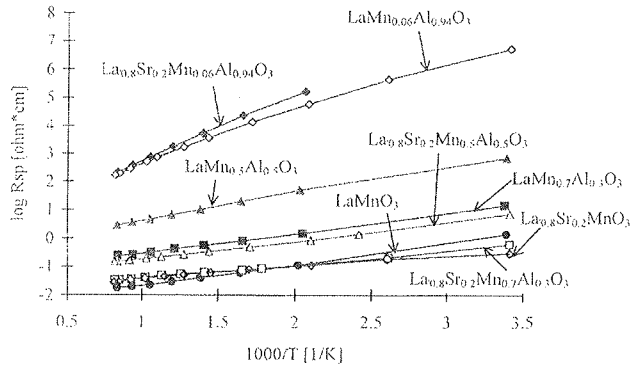


*Fig. 11: Logarithm of resistivity of $La(Mn_{1-x}Al_x)O_3$ and $(La_{0.8}Sr_{0.2})(Mn_{1-x}Al_x)O_3$ vs. reciprocal temperature. Samples with partial exchange of lanthanum with strontium have an extension "S".*

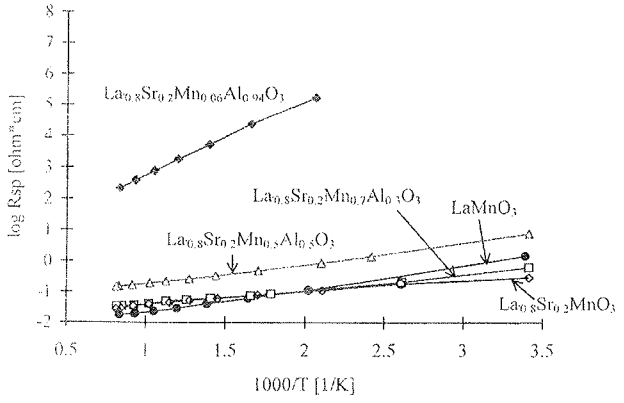


*Fig. 10: Logarithm of resistivity of $(La_{0.8}Sr_{0.2})(Mn_{1-x}Al_x)O_3$ and $LaMnO_3$ vs. reciprocal temperature*

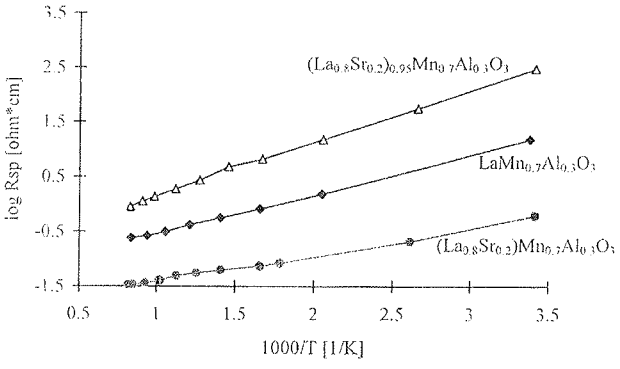


*Fig. 12: The logarithm of specific resistivities vs. reciprocal temperature for $La(Mn_{0.7}Al_{0.3})O_3$, $(La_{0.8}Sr_{0.2})(Mn_{0.7}Al_{0.3})O_3$, and $(La_{0.8}Sr_{0.2})_{0.95}(Mn_{0.7}Al_{0.3})O_3$*

*Table 3. Specific resistivities of stoichiometric and substoichiometric samples at 25 °C, 400 °C, and at 900 °C (Ωcm)*

| Nominal composition | 25°C | 400°C | 900°C |
|---|---|---|---|
| $LaMnO_3$ | 1.4 Ωcm | 0.04 Ωcm | 0.018 Ωcm |
| $La(Mn_{0.7}Al_{0.3})O_3$ | 8.2 Ωcm | 0.57 Ωcm | 0.12 Ωcm |
| $(La_{0.8}Sr_{0.2})(Mn_{0.7}Al_{0.3})O_3$ | 0.62 Ωcm | 0.063 Ωcm | 0.034 Ωcm |
| $(La_{0.8}Sr_{0.2})_{0.95}(Mn_{0.7}Al_{0.3})O_3$ | 280 Ωcm | 4.8 Ωcm | 0.35 Ωcm |

It is interesting to note, however, that the composition with x=0.94 is an exception; namely, the resistivity of the undoped material is lower than the resistivity of the strontium oxide doped one. The reason for this unexpected characteristic is not known yet. The specific resistivities of $La_{0.8}Sr_{0.2}MnO_3$ and $(La_{0.8}Sr_{0.2})(Mn_{0.7}Al_{0.3})O_3$ are nearly temperature independent over the whole measured temperature range.

The logarithm of specific resistivities vs. reciprocal temperature for $(La_{0.8}Sr_{0.2})_{0.95}(Mn_{0.7}Al_{0.3})O_3$. is presented in Fig. 12. Values for $La(Mn_{0.7}Al_{0.3})O_3$, and stoichiometric strontium substituted $(La_{0.8}Sr_{0.2})(Mn_{0.7}Al_{0.3})O_3$ are shown for comparison. The partial exchange of lanthanum with strontium ions significantly decreases the resistivity. However, the resistivities of sub-stoichiometric compositions are higher than those of stoichiometric compositions.

Resistivities for materials with x=0.3, i.e., $La(Mn_{0.7}Al_{0.3})O_3$, $(La_{0.8}Sr_{0.2})(Mn_{0.7}Al_{0.3})O_3$, and substoichiometric $(La_{0.8}Sr_{0.2})_{0.95}(Mn_{0.7}Al_{0.3})O_3$ at room temperature, at 400°C, and at 900°C are summarized in Table III. Data for $LaMnO_3$ are also included for comparision. The partial exchange of lanthanum with strontium ions significantly decreases the resistivity. However, the resistivities of sub-stoichiometric compositions are higher than those of stoichiometric compositions.

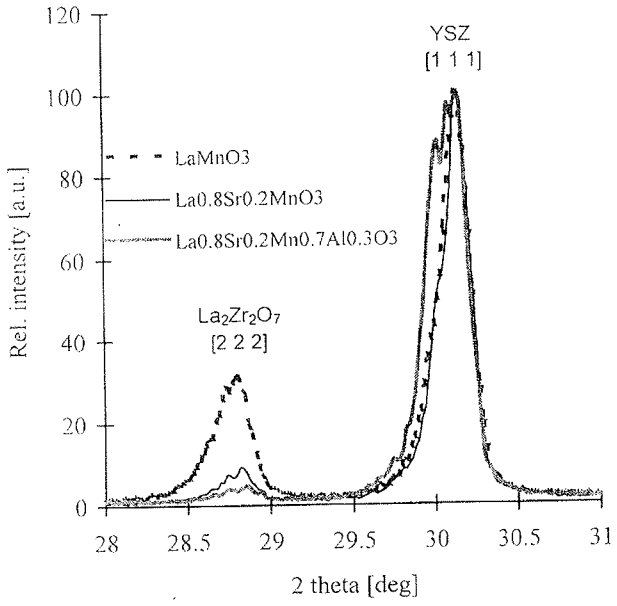


*Fig. 13: Superimposed normalized X-ray spectra of $LaMnO_3$, $(La_{0.8}Sr_{0.2})MnO_3$, and $(La_{0.8}Sr_{0.2})(Mn_{0.7}Al_{0.3})O_3$ mixtures with YSZ after ageing for 300 hours at 1400°C. The [2 2 2] peak of $La_2Zr_2O_7$ at 2 θ=28.8° is shown.*

Superimposed normalized X-ray spectra of $LaMnO_3$, $(La_{0.8}Sr_{0.2})MnO_3$, and $(La_{0.8}Sr_{0.2})(Mn_{0.7}Al_{0.3})O_3$ mixtures with YSZ after ageing for 300 hours at 1400°C, are presented in Fig. 13. The [2 2 2] peak of $La_2Zr_2O_7$ at 2 θ =28.8° is shown. The height of the peak is proportional to the quantity of $La_2Zr_2O_7$ pyrochlore phase which is formed during ageing. The results - the heights of the peaks - indicate that more pyrochlore phase is formed under the same ageing conditions between $LaMnO_3$ and YSZ than between $(La_{0.8}Sr_{0.2})MnO_3$ and YSZ. In the case of $(La_{0.8}Sr_{0.2})(Mn_{0.7}Al_{0.3})O_3$ the quantity of $La_2Zr_2O_7$ was minimized. It is known that the limited exchange of lanthanum oxide with alkaline earth oxides inhibits the formation of $La_2Zr_2O_7$ (see, for example, Ref. /18/. The results showed that the combination of strontium and aluminum oxide further depresses the formation of the undesirable high resistivity pyrochlore phase. No difference between $(La_{0.8}Sr_{0.2})(Mn_{0.7}Al_{0.3})O_3$ and substoichiometric $(La_{0.8}Sr_{0.2})_{0.95}(Mn_{0.7}Al_{0.3})O_3$ was observed.

## CONCLUSIONS

Perovskites with nominal compositions $La(Mn_{1-x}Al_x)O_3$ and strontium doped $(La_{0.8}Sr_{0.2})(Mn_{1-x}Al_x)O_3$ (for x between 0 and 0.94) were synthesized as possible solid oxide fuel cells (SOFC) cathode materials. Some results on substoichiometric $(La_{0.8}Sr_{0.2})_{0.95}(Mn_{0.7}Al_{0.3})O_3$ were also obtained.

The microstructures of alumina substituted materials are porous and average grain diameters decrease with increasing $Al_2O_3$ content. $(La_{0.8}Sr_{0.2})(Mn_{1-x}Al_x)O_3$ perovskites are more densely sintered that those without strontium. Substoichiometry on "A" sites increases the sintered density.

From X-ray diffraction analysis data cell parameters were calculated. The cell volume of $La(Mn_{1-x}Al_x)O_3$ linearly decreases with increasing alumina content from x=0 to x=0.4 which is the limit of solid solubility of $LaAlO_3$ in $LaMnO_3$. Strontium substituted perovskites have smaller cell volumes as their counterparts with the same aluminum / manganese ratio.

Specific resistivities of $La(Mn_{1-x}Al_x)O_3$ increase with increasing concentration of $Al_2O_3$. The resistivities of $LaMnO_3$ and $(La_{0.8}Sr_{0.2})(Mn_{1-x}Al_x)O_3$ for x=0 and 0.3 are nearly the same for the whole temperature range at temperatures above 200°C, whereas for x=0.5 the resistivity is higher by an order of magnitude. The resistivities of strontium doped $(La_{0.8}Sr_{0.2})(Mn_{1-x}Al_x)O_3$ are about one order of magnitude lower than those of undoped samples. The resistivities of sub-stoichiometric compositions are higher than those of stoichiometric compositions.

To study the formation rate of the undesirable high resistive pyrochlore phase $La_2Zr_2O_7$, perovskites and YSZ mixtures were fired at elevated temperatures. The results showed that the combination of strontium and aluminum oxide significantly depress the formation of $La_2Zr_2O_7$. No difference between stoichiometric and substoichiometric materials was detected.

From described results it could be concluded that the optimized composition for SOFC cathodes is $(La_{0.8}Sr_{0.2})(Mn_{0.7}Al_{0.3})O_3$. It's resistivity is similar to $LaMnO_3$ while the reaction rate with YSZ is minimized.

## ACKNOWLEDGEMENTS

This work was performed within the project "New SOFC Materials and Technology; JOU2-CT92-0063". The authors would like to express their thanks to Dr. Toma' Kosmač for helpful discussions. The financial support of the Ministry of Science and Technology of Slovenia is gratefully acknowledged.

## REFERENCES

/1/ W. R. Grove, On voltaic series and the combination of gases by platinum, Phil. Mag., S.3., 14, (86), (1839), 127-130

/2/ N. Q. Minh, Ceramic fuel cells, J. Am. Ceram. Soc., 76, (3), (1993), 563-588

/3/ B. C. H. Steele, State-of-the-art SOFC ceramic materials, Proc. 1 st European Solid Oxide Fuel Cell Forum, European Fuel Cell Group, Ltd. and IEA Advanced Fuel Cell Programme, (Ed. U. Bossel), Lucerne, 1994, 375-397

/4/ K. Ledjeff, T. Rohrbach, G. Schaumberg, Internal reforming for solid oxide fuel cells, Proc. 2nd Int. Symp. on Solid Oxide Fuel Cells, Commission of the European Communities (Ed. F. Grosz, P. Zegers, S. C. Singhal, O. Yamatoto), Athens, 1991, 323-333

/5/ P. Stonehart, The unique features of the solid oxide fuel cell in a hydrocarbon energy world, Proc. 1 st European Solid Oxide Fuel Cell Forum, European Fuel Cell Group, Ltd. and IEA Advanced Fuel Cell Programme, (Ed. U. Bossel), Lucerne, 1994, 15-41

/6/ T. Aida, A. Abudula, M. Ihara, H. Komiyama, K. Yamada, Direct oxidation of methane on anode of solid oxide fuel cell, Proc. 4th Int. Symp. on Solid Oxide Fuel Cells, The Electrochemical Society, Inc. (Ed. M.Dokiya, O.Yamamoto, H. Tagawa, S.C. Singhal), Yokohama, 1995, 801-809

/7/ K. Kendall, Ceramics in fuel cells, Cer. Bull., 70, (7), (1991), 1159-1160

/8/ F. Gross, Solid oxide fuel cells R&D in Europe, Proc. 2nd Int. Symp. on Solid Oxide Fuel Cells, Commission of the European Communities (Ed. F. Grosz, P. Zegers, S. C. Singhal, O. Yamatoto), Athens, 1991, 7-2

/9/ M. Mogensen, N. Christiansen, Fuel cells - familiar principles for electricity generation, Europhys. News, 24, (1993), 7-9

/10/ H. Tagawa, Status of SOFC development in Japan, Proc. 3rd Int. Symp. on Solid Oxide Fuel Cells, The Electrochemical Society, Inc. (Ed. S. C. Singhal, H. Iwahara), Honolulu, 1993, 6-15

/11/ S. Kartha, P. Grimes, Fuel cells: energy conversion for the next century, Physics Today, 47, (11), (1994), 54-61

/12/ A. Mackor, T. P. M. Koster, J. G. Kraaijkamp, J. Gerretsen, Influence of La-substitution and -substoichiometry on conductivity, thermal expansion and chemical stability of Ca- or Sr-doped lanthanum manganites as SOFC cathodes, Proc. 2nd Int. Symp. on Solid Oxide Fuel Cells, Commission of the European Communities (Ed. F. Grosz, P. Zegers, S. C. Singhal, O. Yamatoto), Athens, 1991, 463-471

/13/ J. Gerretsen, A. Mackor, J. P. G. M. van Eijk, T. P. M. Koster, Standardization of thermal expansion coefficient (TEC) measurements for testing the compatibility of SOFC components, Proc. 2nd Int. Symp. on Solid Oxide Fuel Cells, Commission of the European Communities (Ed. F. Grosz, P. Zegers, S. C. Singhal, O. Yamatoto), Athens, 1991, 159-166

/14/ M. Hrovat, S. Bernik, J. Holc, D. Kolar, B. Dacar, Preliminary data on subsolidus phase equilibria in the $La_2O_3$ - $Cr_2O_3$ - $Y_2O_3$ and $La_2O_3$ - $Cr_2O_3$ - $ZrO_2$ systems, J. Mater. Sci. Lett., 14, (23), (1995), 1684-1687

/15/ H. Taimatsu, K. Wada and H. Kaneko, Mechanism of reaction between lanthanum manganite and yttria stabilized zirconia, J. Am. Ceram. Soc., 75 (2), (1992), 401-405

/16/ J. A. M. van Roosmalen and E. H. P. Cordfunke, Chemical reactivity and interdiffusion of (La,Sr)$MnO_3$ and (Zr,Y)$O_2$ solid oxide fuel cell cathode and electrolyte materials, Solid State Ionics, 52 , (1992), 303 - 312

/17/ J. A. Labrincha, J. R. Frade and F. M. B. Marques, $La_2Zr_2O_7$ formed at ceramic electrode/YSZ contacts, J. Mater. Sci. 28, (14), (1993), 3809-3815

/18/ G. Stochniol, E. Syskakis, A. Naoumidis, Compatibility studies between $La_{1-x}Sr_xMnO_3$ and 8YSZ, Proc. 5th IEA Workshop on SOFC, Materials, Process Engineering and Electrochemistry (Eds. P. Biederman, B. Krahl-Urban), Jülich FRG, 1993, 25-31

/19/ D. Kuščer, J. Holc, M. Hrovat, S. Bernik, Z. Samardžija, D. Kolar, Interactions between thick film $LaMnO_3$ SOFC cathode and $ZrO_2$ (8% $Y_2O_3$) during high temperature ageing, Solid State Ionics, 78, (1995), 79-85

/20/ F. W. Poulsen, N. van der Puil, Phase relations and conductivity of Sr- and La-zirconates, Solid State Ionics, 53-56, (pt. 2), (1992), 777-783

/21/ M. Hrovat, J. Holc, D. Kuščer, Z. Samardžija, S. Bernik, Preliminary data on subsolidus phase equilibria in the $La_2O_3$ - $Al_2O_3$ - $Mn_2O_3$ and $La_2O_3$ - $Al_2O_3$ - $Fe_2O_3$ systems, J. Mater. Sci. Lett., 14, (4), (1995), 265-267

/22/ A. Hammouche, E. Siebert, A. Hammou, Crystallographic, thermal and electrochemical properties of the system $La_{1-x}Sr_xMnO_3$ for high temperature solid electrolyte fuel cells, Mat. Res. Bull., 24, (3), (1989), 367-380

*mag. Danjela Kuščer, dipl.ing.*
*dr. Janez Holz, dipl.ing.*
*dr. Marko Hrovat, dipl.ing.*
*dr. Slavko Bernik, dipl.ing.*
*dr. Drago Kolar, dipl.ing.*
*Jožef Stefan Institute*
*Jamova 39, 1000 Ljubljana, Slovenia*
*tel.: +386 61 1773418*
*fax: +386 61 1261029*

*Prispelo (Arrived): 25.3.1997* *Sprejeto (Accepted): 6.5.1997*